DEPENDENCE OF PARTICLE RAPIDITY DISTRIBUTION ON FORWARD ENERGY AND MULTIPLICITY IN NUCLEUS–NUCLEUS COLLISIONS AT AGS ENERGY

Fu-Hu Liu

Institute of Modern Physics and Department of Physics
Shanxi Teachers University
Linfen, Shanxi 041004, China
e-mail: liufh@dns.sxtu.edu.cn

(Received June 21, 2001; revised version received August 9, 2001)

The rapidity distributions of particles produced in nucleus–nucleus (Au–Au) collisions at the Alternating Gradient Synchrotron (AGS) energy (11–15A GeV) have been analyzed by the thermalized cylinder model and the three-fireball model. It is shown that the two models are successful at the AGS energy. The normalized rapidity distributions of produced particles (exclusion of protons) described by the two models do not depend on the forward energy and multiplicity. The rapidity shifts in the two models do not depend on the impact parameter. The proton and deuteron normalized rapidity distributions contributed by the participants in Au-Au collisions do not depend on the forward energy and multiplicity, but the final state proton and deuteron rapidity distributions depend on the forward energy and multiplicity due to the contributions of spectators.

PACS numbers: 25.75.–q, 24.10.Pa

1. Introduction

One of the aims of studying high energy nucleus–nucleus collisions is to investigate the mechanism of nuclear reactions. The knowledge of particle production leads to important constraints on the reactions and is of great importance in order to assess. A lot of models [1] have been introduced for high energy nuclear collisions. Among them, the thermal fireball model [2] was used much earlier in comparably low-energy nuclear reactions. Basing on the fireball model, we have developed a thermalized cylinder model [3] and described the rapidity (or pseudorapidity) distributions of relativistic singly charged particles in nucleus–nucleus collisions over an energy range from a few A GeV to $100A$ TeV [3,4]. It is shown that the thermalized cylinder model is successful in the description of rapidity distributions. On the other hand, basing on the three-fireball model for hadron–hadron collisions [5,6], we have developed a three-fireball model for nucleus–nucleus collisions [7] and described the particle production in nucleus–nucleus collisions at high energy. The three-fireball model is also successful in the description of rapidity distributions.

Many models [1] have been introduced to describe the rapidity distribution of produced particles in high-energy nucleus–nucleus collisions. However, the different models give very different calculated results for proton rapidity distribution. The rapidity distribution of protons produced in nucleus–nucleus collisions is very different from that of other produced particles. The calculated results for proton rapidity distribution by different models are not corresponding to each other. It is necessary to study the proton rapidity distribution in nucleus–nucleus collisions by the thermalized cylinder model and the three-fireball model. The study should be based on the successful description of other produced particle rapidity distribution.

The aim of the present work is to perform a systematic analysis of pions, kaons, protons and deuterons production in nucleus–nucleus collisions at the AGS energy within the thermalized cylinder model and the three-fireball model. The rapidity distributions of the above particles produced in different event groups are calculated and compared with the recent experimental data of the E802 Collaboration [8].

2. The model

2.1. Thermalized Cylinder Model (TCM)

Let us consider the simplest pictures of the one-dimensional string model [9] and the fireball model [2]. In a high-energy nucleon–nucleon collision, a string is formed consisting of two endpoints acting as energy reservoirs and the interior with constant energy per length. Because of the asymmetry of the mechanism, the string will break into many substrings along the direction of the incident beam. The distribution length of substrings will define the width of the pseudorapidity distribution. According to the fireball model, the incident nucleon penetrates through the target nucleon, then a firestreak is formed along the direction of the incident beam. The length of the firestreak will define the width of pseudorapidity distribution. In high-energy nucleus–nucleus collisions, many strings or firestreaks are formed along the incident direction. Finally, a thermalized cylinder is formed because these strings or firestreaks stack and exchange their momentums in the transverse direction.

In a given reference frame, we assume that the thermalized cylinder formed in nucleus–nucleus collisions is in the rapidity range $[y_{\rm min}, y_{\rm max}]$. The emission points with the same rapidity, y_x, in the thermalized cylinder form a cross section (emission source) in the rapidity space. For the thermalized cylinder, the initial extension of the nuclei is not important because of the Lorentz-contraction.

Under the assumption that the particles are emitted isotropically in the rest frame of the emission source, we know that the pseudorapidity (η) distribution of the particles produced in the emission source with rapidity y_x in the concerned reference frame is

$$f(\eta, y_x) = \frac{1}{2\cosh^2(\eta - y_x)} \, . \tag{1}$$

If $y_x = y_{\rm min}$ or $y_{\rm max}$, Eq. (1) will describe the η distributions of leading target or projectile participant nucleons.

In final state, the η distribution of singly charged produced particles (exclusion of protons) is contributed by the whole thermalized cylinder. We have the normalized η distribution of produced particles

$$f_{\rm TCM}(\eta) = \frac{1}{y_{\rm max} - y_{\rm min}} \int\limits_{y_{\rm min}}^{y_{\rm max}} f(\eta, y_x) dy_x \, . \tag{2}$$

The η distribution of protons is contributed by the whole thermalized cylinder and the leading protons. We have the η density distribution of protons

$$\begin{aligned} F_{\rm TCM}(\eta) \;=\; & \frac{(1 - K_{\rm TCM})(N_{\rm TP} + N_{\rm PP})}{y_{\rm max} - y_{\rm min}} \int\limits_{y_{\rm min}}^{y_{\rm max}} f(\eta, y_x) dy_x + K_{\rm TCM}\Big[N_{\rm TP} f(\eta, y_{\rm min}) \\ & + N_{\rm PP} f(\eta, y_{\rm max})\Big] + N_{\rm TS} f(\eta, y_{\rm TS}) + N_{\rm PS} f(\eta, y_{\rm PS}) \, , \end{aligned} \tag{3}$$

where $N_{\rm TP}$, $N_{\rm PP}$, $N_{\rm TS}$, and $N_{\rm PS}$ denote the numbers of protons produced in Target Participant (TP), Projectile Participant (PP), Target Spectator (TS), and Projectile Spectator (PS), respectively. $K_{\rm TCM}$ is the probability of participant proton appearing as a leading particle. $y_{\rm TS}$ and $y_{\rm PS}$ are the mean rapidities of target and projectile spectators, respectively. In the above discussion, we have used the picture of spectator-participant model [10]. The rapidity y can be obtained by the above formulas due to $y \approx \eta$ at high energy [11].

Let y_C denote the midrapidity of produced particles. We have

$$y_{\min} = y_C - \Delta y\,, \tag{4}$$
$$y_{\max} = y_C + \Delta y\,, \tag{5}$$
$$y_{\mathrm{TS}} = y_C - Dy \approx y_{\mathrm{Target}}\,, \tag{6}$$

and

$$y_{\mathrm{PS}} = y_C + Dy \approx y_{\mathrm{Projectile}}\,, \tag{7}$$

where Δy and Dy are the rapidity shifts in the TCM, y_{Target} and $y_{\mathrm{Projectile}}$ are the rapidities of target and projectile, respectively. Generally speaking, y_C should be the rapidity of the center-of-mass system of collisions, the peak position of particle rapidity distribution, or the mean value of particle rapidities.

There are two parameters, Δy and K_{TCM}, in the TCM discussed above. For pions and kaons rapidity we need only one parameter, Δy. The values of N_{TP}, N_{PP}, N_{TS}, and N_{PS} can be obtained by nuclear geometry in concerned nucleus–nucleus collisions.

In the above discussion, the normalization conditions for Eqs. (2) and (3) are

$$\int f_{\mathrm{TCM}}(\eta)d\eta = \int \frac{1}{N}\frac{dN}{d\eta}d\eta = 1\,, \tag{8}$$

and

$$\int F_{\mathrm{TCM}}(\eta)d\eta = \int \frac{1}{N_{\mathrm{EV}}}\frac{dN}{d\eta}d\eta = N_{\mathrm{TP}} + N_{\mathrm{TS}} + N_{\mathrm{PP}} + N_{\mathrm{PS}} \le Z_{\mathrm{T}} + Z_{\mathrm{P}}\,, \tag{9}$$

respectively, where N and N_{EV} are the numbers of particles and events, and Z_{T} and Z_{P} are the atomic numbers of the target and projectile nuclei, respectively. If we consider the production of nucleon cluster in the spectator, the left side of Eq. (9) should be less than $Z_{\mathrm{T}} + Z_{\mathrm{P}}$ due to the decreasing of N_{TS} and N_{PS}.

In the thermalized cylinder formed in high energy nuclear collisions, the excitation degrees of different emission sources may be different. It is expected that the emission sources at and around the midrapidity have a high excitation. The emission sources at and around the rapidity $y_{\min}$ or $y_{\max}$ have a low excitation. As the first approximation, we divide the thermalized cylinder into three parts along the long direction. The middle part is in the rapidity range from $y_C - \frac{1}{3}\Delta y$ to $y_C + \frac{1}{3}\Delta y$ and stays in a high excitation state. The other two parts are in the rapidity range from $y_{\min}$ to $y_C - \frac{1}{3}\Delta y$ and $y_C + \frac{1}{3}\Delta y$ to $y_{\max}$, respectively, and stay in a low excitation state. Because of the relativity, the other two parts have the same excitation degree.

The three parts have the same contribution to the number of final state particles. In the rest frame of the emission source, we assume that the three components of particle momentum obey Gaussian distribution and have the same standard deviation. Then the transverse momentum $P_{\rm t}$ obeys Rayleigh distribution. The transverse mass $m_{\rm t}$ can be obtained by $m_{\rm t} = \sqrt{P_{\rm t}^2 + m_0^2}$, where m_0 is the rest mass of concerned particle.

2.2. Three-Fireball Model (TFM)

According to the TFM [5,6] in high energy hadron–hadron collisions, we have developed a three-fireball model [7] to describe the particle production in high energy nucleus–nucleus collisions. In a high energy hadron–hadron collision, the incident hadron collides with the target. Then a projectile fireball, a central fireball and a target fireball are formed [5,6]. In high energy nucleus–nucleus collisions, many projectile nucleons collide with many target nucleons. For each nucleon–nucleon collision, three fireballs are formed. There are many projectile fireballs, central fireballs and target fireballs in high energy nucleus–nucleus collisions. In rapidity space, the projectile fireballs are in high rapidity region, the central fireballs are in middle rapidity region, and the target fireballs are in low rapidity region. We regard the projectile fireballs formed in nucleus–nucleus collisions as a big projectile fireball, and name it the projectile fireball P^*. Similarly, we regard the central fireballs and the target fireballs formed in nucleus–nucleus collisions as a big central fireball and a big target fireball, and name them the central fireball C^* and the target fireball T^*, respectively.

Each fireball (P^*, C^*, or T^*) is assumed to be isotropic emission in the fireball rest frame. Let y_i denote the rapidity of fireball i^* ($i^* = P^*$, C^*, or T^*) in the concerned reference frame. Replacing y_x by y_i in Eq. (1), the η distribution of the particles produced in the fireball i^* in the concerned reference frame can be given.

In final state, the η distribution of singly charged produced particles (exclusion of protons) is contributed by the three fireballs with the same probability. We have the normalized η distribution of produced particles

$$f_{\rm TFM}(\eta) = \tfrac{1}{3}\Big[f(\eta, y_C) + f(\eta, y_{\rm T}) + f(\eta, y_{\rm P})\Big]\,. \qquad (10)$$

The η distribution of protons is contributed by the three fireballs and the leading protons. We have the η density distribution of protons

$$\begin{aligned} F_{\rm TFM}(\eta) \;=\; & (1 - K_{\rm TFM})(N_{\rm TP} + N_{\rm PP}) f(\eta, y_C) + K_{\rm TFM}\Big[N_{\rm TP} f(\eta, y_{\rm T}) \\ & + \; N_{\rm PP} f(\eta, y_{\rm P})\Big] + N_{\rm TS} f(\eta, y_{\rm TS}) + N_{\rm PS} f(\eta, y_{\rm PS})\,, \end{aligned} \qquad (11)$$

where $K_{\rm TFM}$ is the probability of target or projectile participant proton appearing in the fireball T^* or P^*. The rapidity y can be obtained by Eqs. (10) and (11) due to $y \approx \eta$ at high energy [11].

The parameter y_C in the TFM is in fact the same as that in the TCM. The relationships between $y_{\rm T}$, $y_{\rm P}$ and y_C are

$$y_{\rm T} = y_C - \delta y\,, \tag{12}$$

and

$$y_{\rm P} = y_C + \delta y\,, \tag{13}$$

where δy is the rapidity shift in the TFM. The relationships between $y_{\rm TS}$, $y_{\rm PS}$ and y_C are the same as those in the TCM.

There are two parameters, δy and $K_{\rm TFM}$, in the TFM discussed above. For pions and kaons rapidity we need only one parameter, δy. The values of y_C, $N_{\rm TP}$, $N_{\rm PP}$, $N_{\rm TS}$, and $N_{\rm PS}$ are the same as those in the TCM. The normalization conditions for Eqs. (10) and (11) are the same as those for Eqs. (2) and (3), respectively.

It is expected that the fireball C^* stays in a high excitation state, and the fireballs T^* and P^* stay in a low excitation state. Because of the relativity, the fireballs T^* and P^* have the same excitation degree. In the rest frame of the emission source, we assume that the three components of particle momentum obey Gaussian distribution and have the same standard deviation. In the descriptions of transverse momentum and transverse mass, the TFM has the same idea as those in the TCM. But the emission sources in the TFM and TCM have different rapidities.

3. Comparison with experimental data

Figure 1 presents the rapidity distributions of positive pions (π^+) produced in Au–Au collisions at 11.6A GeV (*i.e.* the AGS energy). The different symbols are the experimental data for the different centrality cuts [8]. The centrality is determined by the value of $E_{\rm ZCAL}$, *i.e.* the energy deposited into the zero-degree calorimeter in the experimental layout of the E802 (E866) Collaboration [8]. Corresponding to the centrality cuts from 0–3% to 43–76%, the $E_{\rm ZCAL}$ range in GeV are 0–240, 240–390, 390–570, 570–780, 780–1020, 1020–1290, 1290–1590, and 1590–3000, respectively [8]. In order to see a clear outline, the dN/dy data presented in Fig. 1 for the different centrality cuts are scaled by adding different constants. The dashed and dotted curves in the figure are our calculated results by the TCM and TFM, respectively. In the calculation, we take a unique $\Delta y = 0.80$ in the TCM and $\delta y = 0.60$ in the TFM to fit the experimental data for the different centrality cuts. The method of χ^2 testing is used in the selection of Δy and δy. The calculated results are scaled to the experimental data.

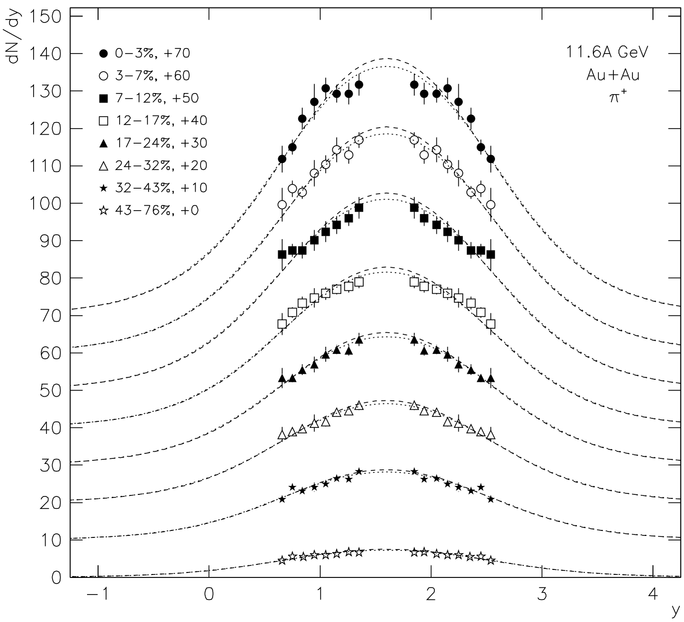

Fig. 1. Rapidity distributions of π^+ in 11.6A GeV Au–Au collisions for different centrality cuts. The different symbols are the experimental data for the different centrality cuts [8]. The left side points about mid-rapidity ($y_C = 1.6$) are the measured data, and the right side points are the data reflected about mid-rapidity. The dashed and dotted curves are our calculated results by the TCM and TFM, respectively. For the centrality cuts from 0-3% to 43-76%, the values of χ^2/Degrees Of Freedom (DOF) in the TCM fits are 0.57, 0.42, 0.62, 0.55, 0.29, 0.28, 0.61, and 0.75, respectively. The corresponding values in the TFM fits are 0.46, 0.38, 0.41, 0.52, 0.21, 0.25, 0.63, and 0.48, respectively.

Figure 2 presents the rapidity distributions of positive kaons (K^+) produced in Au–Au collisions at 11.6A GeV. The meanings of symbols and curves in Fig. 2 are the same as those in Fig. 1. In order to see a clear outline, the dN/dy data presented in Fig. 2 for the different centrality cuts are scaled by adding different constants. In the calculation, we take the same Δy (=0.80) and δy (=0.60) as those for Fig. 1 for the different centrality cuts. The calculated results are scaled to the experimental data.

From Figs. 1 and 2 one can see that the TCM and TFM give a good description of π^+ and K^+ rapidity distributions in Au–Au collisions at the AGS energy. In the calculation for normalized π^+ and K^+ rapidity distributions, we need only one parameter Δy in the TCM, and one parameter δy in the TFM. The values of Δy and δy do not depend on the impact parameter (centrality).

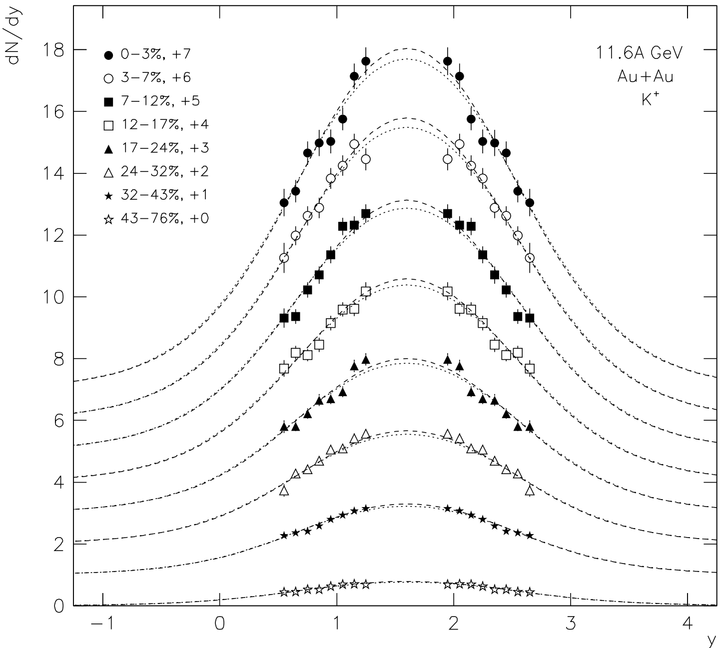

Fig. 2. As for Fig. 1, but showing the results for K^+. For the centrality cuts from 0–3% to 43–76%, the values of χ^2/DOF in the TCM fits are 0.78, 0.64, 0.72, 0.44, 0.48, 0.33, 0.38, and 0.35, respectively. The corresponding values in the TFM fits are 0.61, 0.73, 0.49, 0.56, 0.39, 0.35, 0.68, and 0.40, respectively.

In order to test the TCM and TFM in detail, the π^+ rapidity distributions in Au–Au collisions at 11.6A GeV for different event groups selected by the deposited energy ($E_{\rm ZCAL}$, the forward energy) in the zero-degree calorimeter and the total measured multiplicity ($M_{\rm NMA}$) in the new multiplicity array [8] are given in Fig. 3. The different symbols (letters) are the experimental data for the different groups of $E_{\rm ZCAL}$ and $M_{\rm NMA}$ [8]. In terms of ($E_{\rm ZCAL}$ range, $M_{\rm NMA}$ range), the corresponding borders for the double-event selection using $E_{\rm ZCAL}$ (in GeV) and $M_{\rm NMA}$ for the event groups from (a) to (i) are (0–240, >375), (0–240, 345–375), (0–240, <345), (240–390, >340), (240–390, 305–340), (240–390, <305), (390–570, >295), (390–570, 265–295), and (390–570, <265), respectively. In order to see a clear outline, the dN/dy data presented in Fig. 3 for the event groups from (a) to (i) are scaled by adding different constants. The dashed and dotted curves in the figure are our calculated results by the TCM and TFM, respectively. In the calculation, we take the same Δy (=0.80) and δy (=0.60) as those for Figs. 1 and 2 for the different event groups. The calculated results are scaled to the experimental data.

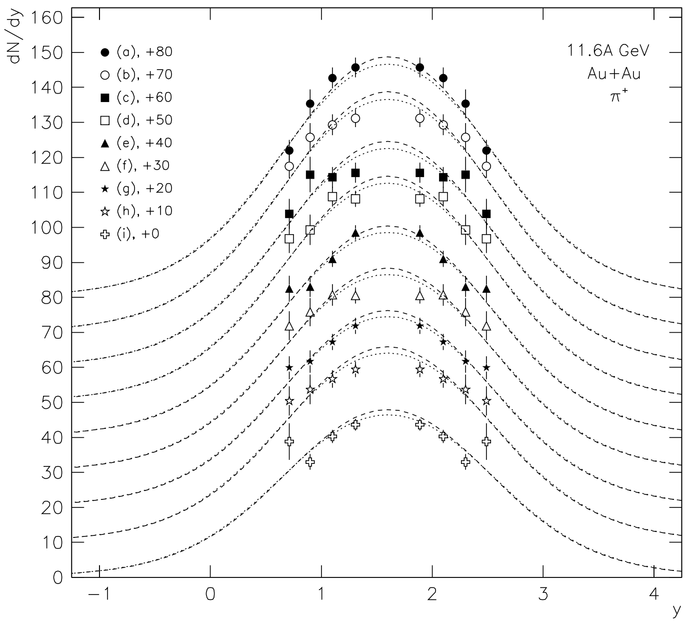

Fig. 3. Rapidity distributions of π^+ in 11.6A GeV Au–Au collisions for different event groups selected by forward energy and multiplicity. The different symbols are the experimental data for the different groups of $E_{\rm ZCAL}$ and $M_{\rm NMA}$ [8]. The left side points about mid-rapidity are the measured data, and the right side points are the data reflected about mid-rapidity. The dashed and dotted curves are our calculated results by the TCM and TFM, respectively. For the event groups from (a) to (i), the values of χ^2/DOF in the TCM fits are 0.24, 0.53, 0.84, 0.61, 0.37, 0.75, 0.36, 0.63, and 1.15, respectively. The corresponding values in the TFM fits are 0.37, 0.39, 0.62, 0.54, 0.37, 0.53, 0.26, 0.42, and 0.96, respectively.

Figure 4 is similar to Fig. 3, but it shows the K^+ rapidity distribution in Au–Au collisions at 11.6A GeV. In order to see a clear outline, the dN/dy data presented in Fig. 4 for the different event groups are scaled by adding different constants. In the calculation, we take the same Δy and δy as those for Figs. 1–3 for the different event groups. The calculated results are scaled to the experimental data.

From Figs. 3 and 4 one can see that the TCM and TFM essentially reproduce the π^+ and K^+ rapidity distributions in 11.6A GeV Au–Au collisions for different event groups. The only parameter Δy in the TCM and δy in the TFM do not depend on the selection of events.

The correlation between $\langle m_{\rm t}\rangle - m_0$ and y for π^+ produced in Au–Au collisions at 11.6A GeV is shown in Fig. 5. The centrality cuts corresponding to the different experimental data (points) [8] are noted in the figure. In

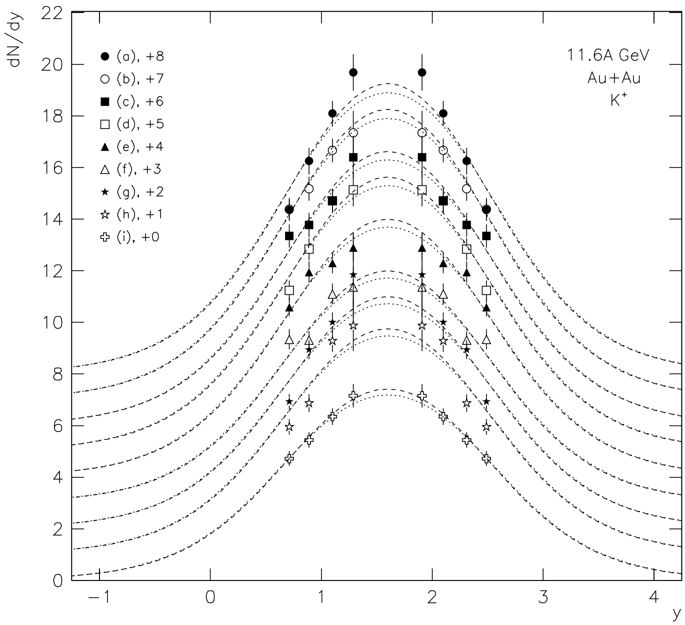

Fig. 4. As for Fig. 3, but showing the results for K^+. For the event groups from (a) to (i), the values of χ^2/DOF in the TCM fits are 1.14, 0.32, 0.65, 0.62, 0.43, 0.81, 1.34, 1.46, and 0.29, respectively. The corresponding values in the TFM fits are 1.34, 0.31, 0.76, 0.72, 0.37, 0.93, 1.33, 1.42, and 0.36, respectively.

order to see a clear outline, the $\langle m_{\rm t}\rangle - m_0$ data presented in Fig. 5 for the different centrality cuts are scaled by adding different constants. The dashed and dotted curves in the figure are our calculated results by the TCM and TFM, respectively. In the calculation, we take the same Δy and δy as those in Figs. 1–4. For the middle part with high excitation in the TCM and the fireball C^* in the TFM, we take $\langle m_{\rm t}\rangle = 0.60$ GeV$/c^2$. For the two parts with low excitation in the TCM and the fireballs T^* and P^*, we take $\langle m_{\rm t}\rangle = 0.18$ GeV$/c^2$. The standard deviations of momentum distribution corresponding to the two values of mean transverse mass are 0.46 and 0.08 GeV$/c^2$, respectively. The method of χ^2 testing is used in the selection of free parameters. The calculated curves are scaled to the data yield.

The correlation between $\langle m_{\rm t}\rangle - m_0$ and y for K^+ produced in Au–Au collisions at 11.6A GeV is shown in Fig. 6. The centrality cuts corresponding to the different experimental data (points) [8] are noted in the figure. In order to see a clear outline, the $\langle m_{\rm t}\rangle - m_0$ data presented in Fig. 6 for the different centrality cuts are scaled by adding different constants. The dashed and dotted curves in the figures are our calculated results by the TCM and TFM, respectively. In the calculation, we take the same Δy and δy as those

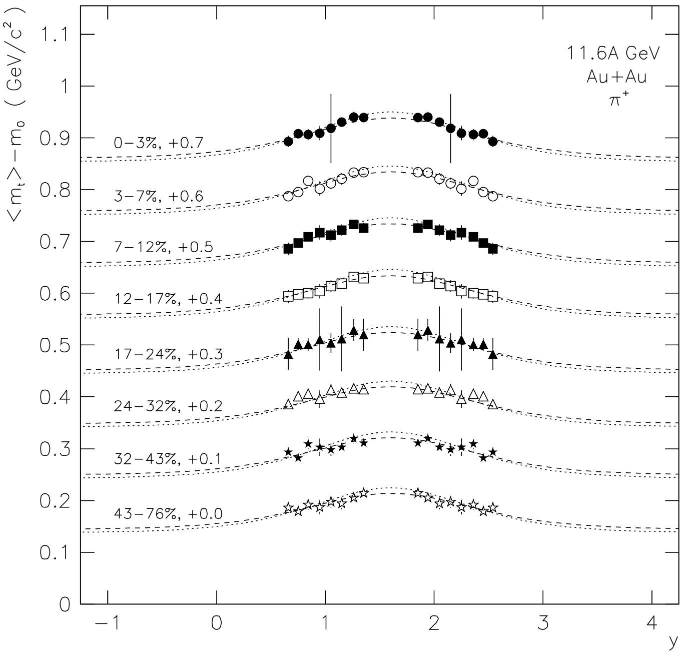

Fig. 5. Correlation between $\langle m_{\rm t}\rangle - m_0$ and y for π^+ in 11.6A GeV Au–Au collisions for different centrality cuts. The different symbols are the experimental data for the different centrality cuts [8]. The left side points about mid-rapidity are the measured data, and the right side points are the data reflected about mid-rapidity. The dashed and dotted curves are our calculated results by the TCM and TFM, respectively. For the centrality cuts from 0-3% to 43-76%, the values of χ^2/DOF in the TCM fits are 0.61, 1.10, 0.54, 0.24, 0.66, 0.93, 0.90, and 0.72, respectively. The corresponding values in the TFM fits are 0.37, 0.89, 0.78, 0.79, 0.66, 1.22, 1.45, and 1.02, respectively.

in Figs. 1–5. For the middle part with high excitation in the TCM and the fireball C^* in the TFM, we take $\langle m_{\rm t}\rangle = 1.60$ GeV/c^2. For the two parts with low excitation in the TCM and the fireballs T^* and P^*, we take $\langle m_{\rm t}\rangle = 0.54$ GeV/c^2. The standard deviations of momentum distribution corresponding to the two values of mean transverse mass are 1.19 and 0.16 GeV/c^2, respectively. The method of χ^2 testing is used in the selection of free parameters. The calculated curves are scaled to the data yield.

From Figs. 5 and 6 one can see that the TCM and TFM give a good description of the correlation between $\langle m_{\rm t}\rangle - m_0$ and y for π^+ produced in different centralities Au–Au collisions at the AGS energy. The TCM and TFM essentially reproduce the correlation between $\langle m_{\rm t}\rangle - m_0$ and y for K^+ produced in the same collisions.

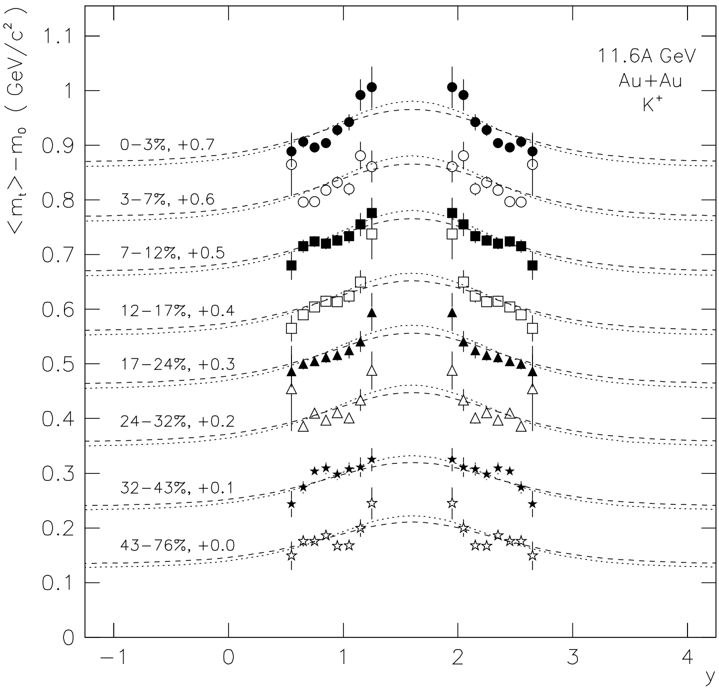

Fig. 6. As for Fig. 5, but showing the results for K^+. For the centrality cuts from 0-3% to 43-76%, the values of χ^2/DOF in the TCM fits are 1.34, 1.24, 0.33, 1.06, 0.45, 1.04, 0.72, and 1.05, respectively. The corresponding values in the TFM fits are 1.18, 1.26, 0.33, 0.89, 0.45, 1.15, 0.60, and 1.20, respectively.

The rapidity distributions of protons (p) produced in different centralities Au–Au collisions at 11.6A GeV [8] are given in Fig. 7. The meanings of symbols and curves in Fig. 7 are the same as those in Figs. 1 and 2. In order to see a clear outline, the dN/dy data given in Fig. 7 for the different centralities (from small impact parameter to great one) are scaled by adding different constants. In the calculation, we take $\Delta y = 0.70$, $\delta y = 0.63$, $K_{\mathrm{TCM}} = 0.75$, and $K_{\mathrm{TFM}} = 0.95$ for the different centrality cuts. In the calculation by using Eqs. (3) and (11), the third parameter is one of N_{TP}, N_{PP}, N_{TS}, and N_{PS}. Generally speaking, we can calculate the third parameter by nuclear colliding geometry at a fixed impact parameter. For the purpose of convenience, we treat the third parameter N_{TP} as a free parameter. Then, for Au–Au collisions, $N_{\mathrm{PP}} = N_{\mathrm{TP}}$, $N_{\mathrm{TS}} = N_{\mathrm{PS}} \leq Z_{\mathrm{T}} - N_{\mathrm{TP}}$. From small impact parameter to great one, the values of N_{TP} are taken as 77, 65, 52, 42, 35, 30, 20, and 6, respectively. Because the calculated curves are scaled to the data yield, the values of N_{TP} and N_{TS} have only the relative meaning. In the calculation, the method of χ^2 testing is used in the selection of free parameters.

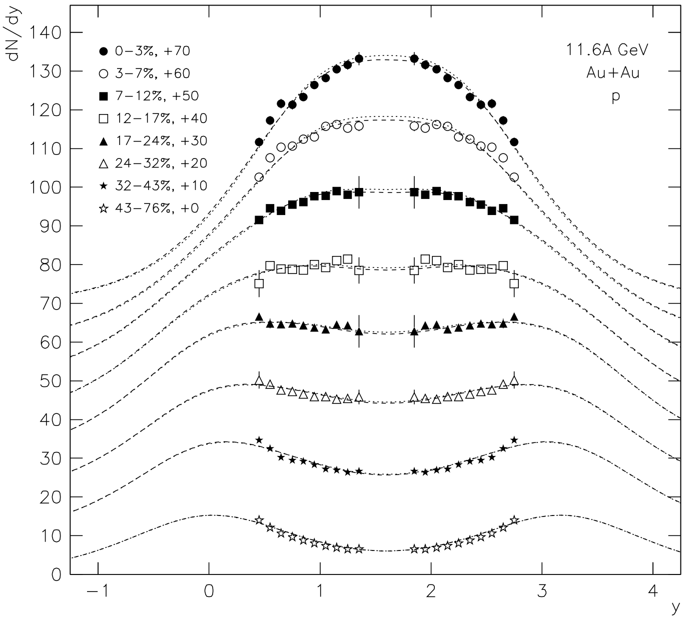

Fig. 7. As for Fig. 1, but showing the results for p. For the centrality cuts from 0-3% to 43-76%, the values of χ^2/DOF in the TCM fits are 0.72, 0.70, 0.28, 0.81, 0.32, 0.30, 0.98, and 1.24, respectively. The corresponding values in the TFM fits are 0.78, 0.72, 0.40, 0.61, 0.44, 0.50, 0.91, and 1.45, respectively.

Figure 8 gives the rapidity distributions of protons in 11.6A GeV Au–Au collisions for different event groups selected by $E_{\rm ZCAL}$ and $M_{\rm NMA}$ [8]. The meanings of symbols and curves in Fig. 8 are the same as those in Figs. 3 and 4. In order to see a clear outline, the dN/dy data given in Fig. 8 for the different event groups are scaled by adding different constants. In the calculation, we take the same Δy, δy, $K_{\rm TCM}$, and $K_{\rm TFM}$ as those for Fig. 7. For the event groups from (a) to (i), the values of $N_{\rm TP}$ are taken as 79, 70, 55, 63, 58, 58, 58, 48, and 45, respectively. Because the calculated curves are scaled to the data yield, the values of $N_{\rm TP}$ and $N_{\rm TS}$ have only the relative meaning. In the calculation, the method of χ^2 testing is used in the selection of free parameters.

Figures 7 and 8 show that the TCM and TFM give a good description of proton rapidity distributions in Au–Au collisions at the AGS energy. The values of Δy, δy, $K_{\rm TCM}$, and $K_{\rm TFM}$ do not depend on the centrality cuts determined by the forward energy and event groups selected by the forward energy and multiplicity. Because the spectators stay in an excitation state, some of protons produced in the spectators may have a greater (or smaller) (pseudo)rapidity than the projectile (or target). We have assumed that the

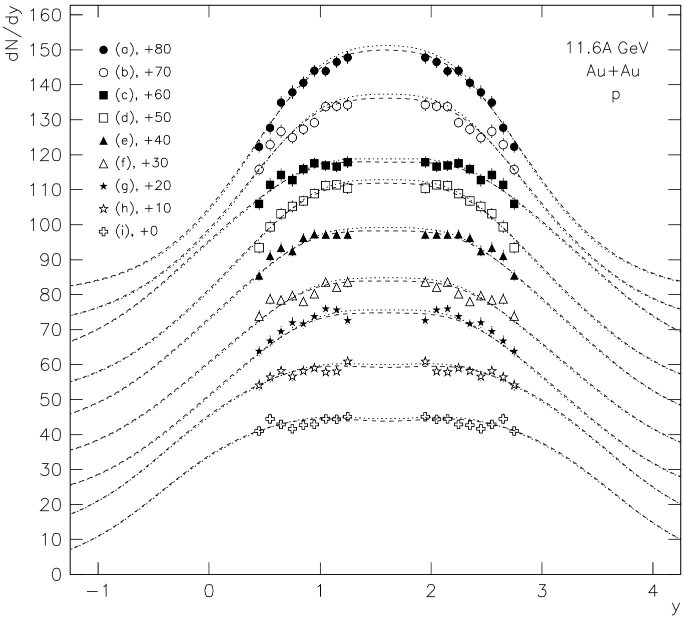

Fig. 8. As for Fig. 3, but showing the results for p. For the event groups from (a) to (i), the values of χ^2/DOF in the TCM fits are 0.36, 0.83, 0.37, 0.37, 0.49, 0.88, 0.86, 0.42, and 0.66, respectively. The corresponding values in the TFM fits are 0.55, 0.99, 0.40, 0.35, 0.56, 1.02, 0.70, 0.65, and 0.71, respectively.

spectator protons are emitted isotropically in the rest frame of the emission source. The mean (pseudo)rapidity of spectator protons is the rapidity of projectile (or target).

Figure 9 is similar to Fig. 7, but it shows the rapidity distribution of deuterons (d) produced in 11.6A GeV Au–Au collisions [8]. In order to see a clear outline, the dN/dy data given in Fig. 9 for the different centrality cuts are scaled by adding different constants. In the calculation, we take the same Δy, δy, $K_{\rm TCM}$, and $K_{\rm TFM}$ as those for Figs. 7 and 8. For the events from small impact parameter to great one, the values of $N_{\rm TP}$ are taken as 79, 50, 40, 10, 10, 5, 0, and 0, respectively. We would like to emphasize again that the values of $N_{\rm TP}$ and $N_{\rm TS}$ have only the relative meaning because the calculated curves are scaled to the data yield.

One can see from Fig. 9 that the TCM and TFM essentially reproduce the deuteron rapidity distributions in 11.6A GeV Au–Au collisions for the centrality cuts from 0–3% to 32–43%. Both the TCM and TFM fail to reproduce the data for the centrality cut of 43–76%. In the peripheral nucleus–nucleus collisions, the spectators have a great contribution to the deuteron rapidity distribution. Both the models have used a too wide rapidity distri-

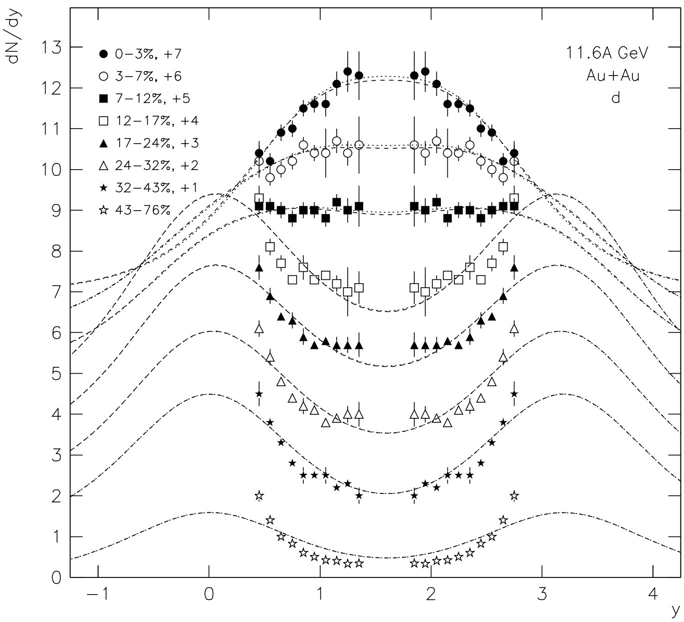

Fig. 9. As for Fig. 1, but showing the results for d. For the centrality cuts from 0-3% to 43-76%, the values of χ^2/DOF in the TCM fits are 0.68, 0.70, 0.39, 1.46, 0.99, 1.33, 1.59, and 16.88, respectively. The corresponding values in the TFM fits are 0.62, 0.66, 0.55, 1.22, 0.89, 1.03, 1.66, and 16.98, respectively.

bution for spectator deuterons. Eq. (1) is the result of an isotropic emission. It approximates to a Gaussian distribution with the standard deviation of 0.91 [12]. We can use a narrower Gaussian to describe the rapidity distribution for spectator deuterons. Using the revised TCM and TFM, we have recalculated the deuteron rapidity distributions in 11.6A GeV Au–Au collisions for different centrality cuts.

Figure 10 presents the deuteron rapidity distribution calculated by the revised TCM and TFM. The experimental data [8] are the same as those in Fig. 9. In the calculation, we have not changed the values of Δy, δy, $K_{\rm TCM}$, and $K_{\rm TFM}$. For the rapidity distribution of spectator deuterons, we use a Gaussian distribution with the standard deviation of 0.40. The values of $N_{\rm TP}$ have been changed from Fig. 9. From small impact parameter to great one, the values of $N_{\rm TP}$ are taken as 79, 65, 55, 40, 34, 25, 18, and 10, respectively. The values of $N_{\rm TP}$ and $N_{\rm TS}$ have only the relative meaning because the calculated curves are scaled to the data yield.

From Fig. 10 one can see that the revised TCM and TFM give a good description of deuteron rapidity distributions in 11.6A GeV Au–Au collisions for different centrality cuts. Comparing Figs. 9 and 10, one may say that the

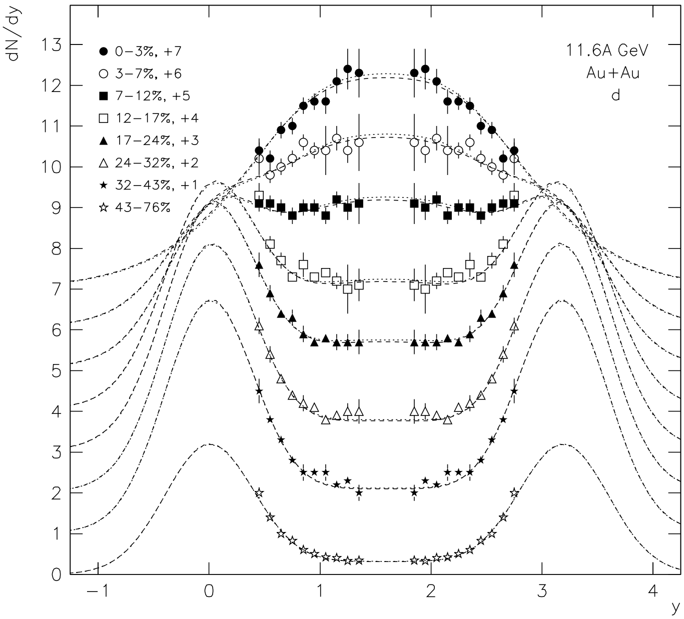

Fig. 10. As for Fig. 9, but showing a comparison between the experimental data [8] and the calculated results by the revised TCM and TFM. For the centrality cuts from 0-3% to 43-76%, the values of χ^2/DOF in the TCM fits are 0.69, 0.44, 0.35, 0.45, 0.39, 0.60, 0.87, and 0.82, respectively. The corresponding values in the TFM fits are 0.56, 0.45, 0.32, 0.94, 0.28, 0.78, 1.05, and 0.88, respectively.

revised TCM and TFM seem better than the original models in the given experimental rapidity region. We have recalculated the proton rapidity distributions (Figs. 7 and 8) by the revised models and obtained acceptable results in the given experimental rapidity region. Because the experimental data do not cover the target and projectile spectator fragmentation regions, it is hard to say that what standard deviation of Gaussian distribution for spectator proton and deuteron rapidity is the best. An isotropic emission gives a Gaussian η ($\approx y$ at high energy [11]) distribution with standard deviation of 0.91 [12]. A width narrower than 0.91 means a transverse flow, while a width wider than 0.91 means a longitudinal flow. The spectator deuteron rapidity distribution in Au–Au collisions at the AGS energy means the existence of a transverse flow. According to Eqs. (3) and (11), if we consider only the contributions of participants in Au–Au collisions, the normalized proton and deuteron rapidity distributions do not depend on the centrality (impact parameter), forward energy, and multiplicity. Exclusion of the spectator's contribution, the distribution shapes of Eqs. (3) and (11) are only determined by Δy and δy, respectively.

From the above comparison and discussion we know that the parameter Δy in the TCM and δy in the TFM do not depend on the centrality (impact parameter), forward energy, and multiplicity. In the words of string model [9] or fireball model [2], the length of string or firestreak formed in Au–Au collisions at the AGS energy does not depend on the centrality (impact parameter), forward energy, and multiplicity.

4. Conclusions and discussions

From the above figures one can see that the TCM and TFM are successful in the descriptions of π^+ and K^+ rapidity distributions in Au–Au collisions at the AGS energy. To describe the normalized rapidity distributions of π^+ and K^+, we need only one parameter, Δy in the TCM, or δy in the TFM. The values of Δy and δy do not depend on the centrality cuts (impact parameter) determined by the forward energy and the event groups selected by the forward energy and multiplicity. The TCM and TFM can also describe the correlation between $\langle m_{\mathrm{t}}\rangle - m_0$ and y for π^+ and K^+ produced in Au–Au collisions at the AGS energy. The (revised) TCM and TFM are also successful in the descriptions of proton and deuteron rapidity distributions in Au–Au collisions at the AGS energy. The proton and deuteron normalized rapidity distributions contributed by the participants do not depend on the forward energy and multiplicity, but the final state proton and deuteron rapidity distributions depend on the forward energy and multiplicity due to the contributions of spectators.

We have also calculated the normalized rapidity distributions for produced particles (exclusion of protons) by the TCM and TFM at the Dubna energy (a few A GeV) and the Super Proton Synchrotron (SPS) energy (60–200A GeV) in our previous work [4,7,13]. It is shown that the TCM and TFM are successful. The values of Δy and δy do not depend on the centrality cuts and event selections at a given incident energy. But the two values increase with increasing the incident energy.

The independence of Δy on centrality shows that the thermalized cylinder formed in nucleus–nucleus collisions is an uniform superposition of strings or firestreaks formed in nucleon–nucleon collisions at the same energy per nucleon. The length of the thermalized cylinder and the width of the rapidity distribution do not depend on the number of participant nucleons [14]. The independence of δy on centrality shows that the three fireballs formed in nucleus–nucleus collisions is an uniform superposition of the three small fireballs formed in nucleon–nucleon collisions at the same energy per nucleon. The distance between the projectile and target fireballs and the width of the rapidity distribution do not depend on the number of participant nucleons.

The values of rapidity shift increase with increasing the incident energy. This renders that the length of the thermalized cylinder (or the distance between the projectile and target fireballs) and the width of the rapidity distribution increase with increasing the incident energy. It is expected that a plateau will appear in the pions (and kaons) rapidity distribution at very high energy [15,16]. The thermalized cylinder model can give a description for the plateau structure in the rapidity distribution if we use a great Δy. But the three-fireball model fails to give such a distribution. Maybe, we can introduce a longitudinal flow in the three-fireball model and describe the plateau structure. It is also expected that a two-peak will appear in the pions (and kaons) rapidity distribution at very high energy [15,16]. A revised thermalized cylinder model (two-cylinder model) can give a description for the two-peak structure. The three-fireball model does not have a revised version to describe the two-peak structure.

Our previous work [4,7,13] shows that the values of Δy and δy are very small (≈ 0.2–0.4) at the Dubna energy. The TCM and TFM can be regarded approximately as a single fireball model. For proton rapidity distribution at the SPS energy, the TCM is successful and the TFM is not successful. It is expected that the TCM will be successful in the description of normalized rapidity distribution for produced particles at the Relativistic Heavy Ion Collider (RHIC) energy ($100A$ GeV + $100A$ GeV) and the TFM will be unsuccessful. At the RHIC energy, a longitudinal flow has to be introduced in the TFM.

This work was supported by the China Scholarship Council, Shanxi Provincial Foundation for Returned Overseas Scholars, Shanxi Provincial Foundation for Leading Specialists in Science, and Shanxi Provincial Science Foundation for Young Specialists.

REFERENCES

[1] J. Geiss, W. Cassing, C. Greiner, *Nucl. Phys.* **A644**, 107 (1998), and references therein.

[2] W.Y. Chang, *Acta Phys. Sin.* **17**, 271 (1961), and references therein; G.D. Westfall *et al.*, *Phys. Rev. Lett.* **37**, 1202 (1976).

[3] F.H. Liu, *Acta Phys. Sin.* (Overseas Edition) **7**, 321 (1998); F.H. Liu, Yu.A. Panebratsev, *Nucl. Phys.* **A641**, 379 (1998); F.H. Liu, Yu.A. Panebratsev, *Phys. Rev.* **C59**, 1798 (1999).

[4] F.H. Liu, Yu.A. Panebratsev, *Phys. Rev.* **C59**, 1193 (1999); F.H. Liu, Yu.A. Panebratsev, *Can. J. Phys.* **77**, 313 (1999); F.H. Liu, *Chin. J. Phys.* **38**, 42 (2000).

[5] A. D'innocenzo, G. Ingrosso, P. Rotelli, *Lett. Nuovo Cimento* **25**, 393 (1979); A. D'innocenzo, G. Ingrosso, P. Rotelli, *Lett. Nuovo Cimento* **27**, 457 (1980); A. D'innocenzo, G. Ingrosso, P. Rotelli, *Nuovo Cimento* **A44**, 375 (1978); A. D'innocenzo, G. Ingrosso, P. Rotelli, *Nuovo Cimento* **A55**, 417 (1980).

[6] L.S. Liu, T.C. Meng, *Phys. Rev.* **D27**, 2640 (1983); K.C. Chou, L.S. Liu, T.C. Meng, *Phys. Rev.* **D28**, 1080 (1983).

[7] F.H. Liu, H.C. Sun, *High Energy Phys. Nucl. Phys.* **19**, 21 (1995); and in Chinese Edition **18**, 1073 (1994).

[8] E802 Collaboration, L. Ahle *et al.*, *Phys. Rev.* **C59**, 2173 (1999); E802 Collaboration, L. Ahle *et al.*, *Phys. Rev.* **C60**, 064901 (1999).

[9] K. Werner, *Phys. Rep.* **232**, 87 (1995).

[10] R.J. Glauber, in *Lectures of Theoretical Physics*, edited by W.E. Brittin and L.G. Dungam, Interscience, New York 1959, Vol. 1, p. 315.

[11] EMU01 Collaboration, M.I. Adamovich *et al.*, *Nucl. Phys.* **A593**, 535 (1995).

[12] EMU01 Collaboration, M.I. Adamovich *et al.*, *Phys. Lett.* **B352**, 472 (1995).

[13] F.H. Liu, *Nuovo Cim.* **A112**, 1167 (1999); F.H. Liu, *Can. J. Phys.* **38**, 907 (2000); F.H. Liu, *Phys. Rev.* **D63**, 032001 (2001).

[14] F.H. Liu, *Acta Phys. Pol.* **B32**, 205 (2001).

[15] M. Derrick, S. Abachi, in *Advanced Series on Directions in High Energy Physics — Vol.2 : Hadronic Multiparticle Production*, edited by P. Carruthers, World Scientific, Singapore 1988, p. 57.

[16] R. Campanini, in *Advanced Series on Directions in High Energy Physics — Vol.2 : Hadronic Multiparticle Production*, edited by P. Carruthers, World Scientific, Singapore 1988, p. 119.